A&A 518, A62 (2010)
DOI: 10.1051/0004-6361/200913660

Astronomy & Astrophysics

Extinction A_V, R towards emission nebulae derived from common upper level Paschen-Balmer hydrogen lines⋆

A. Greve

IRAM, 300 rue de la Piscine, 38406 Saint-Martin d'Hères, France
e-mail: greve@iram.fr

Received 13 November 2009 / Accepted 5 April 2010

ABSTRACT

The reddening in and around emission nebulae is characterized by the extinction A_V and the ratio R of the absolute-to-selective absorption. Both are usually derived from the photometry of a single star or cluster stars that are associated with an emission nebula. Using the parameterized reddening relation published by Cardelli et al. (1989, ApJ, 345, 245), we show that A_V *and* R can be derived with good precision from the observation of a set of common upper level Paschen-Balmer hydrogen line ratios. The use of common upper level line ratios has the advantage of being nearly independent of the excitation condition of the nebula (n_e, T_e). The line ratio method can be applied in regions where no stars are available for photometry.

Key words. dust, extinction

1. Introduction

The reddening in and around emission nebulae is characterized by the extinction A_V (magnitude) and the ratio R of the absolute-to-selective absorption, with $A_V = RE(B-V)$. In interstellar space is $R \approx 3.1$, while in and around emission nebulae – especially when embedded in a molecular cloud (for the Orion nebula see Goudis 1982; O'Dell & Wen 1992) – the value R can be significantly higher, i.e. $R \approx 4$–6. This indicates the presence of dust of a different size and/or composition than in the diffuse interstellar medium (see for instance Whittet 2003; Mathis 1990). The value R is important in studies of both the presence and evolution of dust in/around emission nebulae, while on the practical side the values A_V, R are important for the abundance analysis of elements with lines that cover the UV, visible, and near-IR wavelength region.

The values A_V and R can be derived from the photometry of (cluster) stars, if present and associated with an emission nebula, while the measurement of a few emission line ratios, for instance Hα/Hβ and Hα/Hγ, provide only A_V. We show that the values A_V *and* R can be derived with good precision when applying the parameterized reddening relation derived by Cardelli et al. (1989, CCM) to a set of common upper level Paschen(P)-Balmer(H) hydrogen emission lines. The use of common PH lines has the advantage (1) of covering the near-IR wavelength region 10 938 Å (P 6)–~8500 Å (~P 20) and the blue wavelength region 4102 Å (H 6)–~3700 Å (~H 20), which is sensitive to the particular value R (see Fig. 3 in Cardelli et al. 1989; and Fig. 6 below); (2) of their line ratios being nearly independent of the excitation condition (n_e, T_e) of the nebula (Osterbrock 1989) so that the ratios can be used as a "standard candle" of emission nebulae; and (3) being able to determine A_V and R for emission objects where no stars are available for photometry, as in many galactic and extragalactic emission nebulae, and planetary nebulae. Although the PH-method is elegant in the application of the theoretical line ratios (see Osterbrock 1989), its main disadvantage is the weakness of the lines (Table 5). For this reason, the common upper line ratio method has not been exploited widely, but CCD spectroscopy and large aperture telescopes have changed the situation.

To illustrate the PH-method of A_V, R determination, we analyse hydrogen emission line observations of M 8 and M 17, made with the BC-spectrograph on the ESO 1.52-m telescope, and observations of M 8, M 16, M 17, M 20, M 42, NGC 3603, and S 311, which were obtained from observations with the UVES-spectrograph on one ESO-VLT 8-m telescope and published by Garcia-Rojas et al. (2005, 2006, 2007) and Esteban et al. (2004, M 42). Where possible, we compare the values A_V, R derived from the PH-method with values derived from photometry. In addition, we derive A_V, R of the planetary nebula NGC 7027 (of higher density and temperature than the emission nebulae) from a combination of emission line data published by Rudy et al. (1992) and Zhang et al. (2005).

2. The reddening determination A_V, R

There are three alternative methods for determining A_V and R.

2.1. Photometric method

The photometric determination of A_V, R uses two-colour diagrams of a group of stars (cluster stars) and usually the assumption/condition that the observed stars are reddened main sequence stars. A systematic deviation of the observed colours from the $R = 3.1$ reddening line is interpreted to be caused by dust with a higher value R. The colour diagrams of NGC 6611 stars (M 16) and NGC 6618 stars (M 17) used in this way are shown by Chini et al. (1980), Chini & Krügel (1983), and Chini & Wargau (1990).

⋆ Partially based on observations made at ESO, La Silla.

2.2. Spectro-photometric method

The comparison of (narrow-band) spectro-photometric measurements of a star of known spectral type with its non-reddened energy distribution allows A_V, R to be determined. The spectral bands can be the colours LKHJIRVBU, as used by Cardelli et al. (1989) for deriving the reddening law.

2.3. Paschen-Balmer common line ratio method

The PH common line ratio method uses the parameterized reddening relation published by Cardelli et al. (1989)

$$\langle A(\lambda)/A(V)\rangle = a(x) + b(x)/R, \quad (1)$$

which can be written in the form (see Greve et al. 1994)

$$A_V\,\Delta a + (A_V/R)\Delta b = 2.5\,\log(R_o/R_p). \quad (2)$$

In relation (2), $R_p = I(\mathrm{P}n)/I(\mathrm{H}n)$ is the predicted intensity ratio of the common Paschen-Balmer line pair of quantum level n, while $R_o = F(\mathrm{P}n)/F(\mathrm{H}n)$ is the observed line ratio. The predicted line ratios are taken from Brocklehurst (1971) or Storey & Hummer (1995). It is found that the ratio $R_p(n)$ is a constant within ~±10% for the range of levels n, densities n_e, and temperatures T_e under consideration (Sect. 3). The values $\Delta a(\lambda_{\mathrm{P}n},\lambda_{\mathrm{H}n})$ and $\Delta b(\lambda_{\mathrm{P}n},\lambda_{\mathrm{H}n})$ in relation (2) are derived from the relations $a(x)$, $b(x)$ ($x = 1/\lambda$, 0.3 $\mu\mathrm{m}^{-1} \le x \le$ 3.3 $\mu\mathrm{m}^{-1}$) published by Cardelli et al. The values A_V and R are obtained from a least-square solution when using ~6 to 10 common line pairs in relation (2).

3. Accuracy of the PH-method

The non-reddened and reddened Paschen and Balmer lines follow a smooth decrement and deviations reveal inconsistencies of the observations and/or data reduction. This is important for blended Paschen and Balmer lines (see Table 5). Inconsistencies can be removed, to some extent, by forcing the observations to follow smooth decrements (see Figs. 2 and 3 below), or in case a large number of line pairs has been observed, by leaving out inconsistent data. For the reduction of the selected, and/or "cleaned", set of line ratios we used the least-square method to derive A_V and R, and the uncertainties σ_A and σ_R of the parameter A_V, R (see Bevington & Robinson 2003). We did not apply a weighting to the observations.

To evaluate the accuracy of the PH-method we took the predicted intensities (Case B) of the 8 line pairs $I(\mathrm{P}n), I(\mathrm{H}n)$ between n = 6 (10 938 Å/4103 Å) and n = 13 (8665 Å/3734 Å)[1] and calculated, using relation (1), for these lines the reddened intensities $F(\mathrm{P}n), F(\mathrm{H}n)$ for selected values A_V, R. From these intensities we formed the ratios $R_o(\gamma) = \gamma_n\, F(\mathrm{P}n)/F(\mathrm{H}n)$ in which the random numbers $0.8 \le \gamma_n \le 1.2$ simulate observations of ≲±20% accuracy. The ratios $R_o(\gamma)$ were then used in relation (2) to calculate A_V, R. For a large set of random numbers γ_n we find that the values A_V, R are recovered within 10 to 15% accuracy of the original values.

From the line ratios $R_p = I(\mathrm{P}n)/I(\mathrm{H}n)$ ($8 \le n \le 20$; Case B) published by Osterbrock (1989), Brocklehurst (1971), and Storey & Hummer (1995) it follows that R_p varies by ~±5% for electron densities between $10^2 \lesssim n_e\ [\mathrm{cm}^{-3}] \lesssim 10^4$ and electron temperatures between $5000 \lesssim T_e\ [\mathrm{K}] \lesssim 15\,000$. When using the observed line ratios of M 16 (Garcia-Rojas et al. 2006) and the predicted ratios $R_p = 0.345 \pm 0.017$ (±5%) in relation (2), it is found that the calculated values A_V and R also vary by ±5%. Generally, the accuracy of the PH-method is set by the accuracy of the observations rather than the emission nebula parameter n_e, T_e. For the higher temperature and higher electron density of planetary nebulae the predicted ratio is $R_p \approx 0.31$, i.e approximately 10% lower than for emission nebulae (see Osterbrock 1989; Storey & Hummer 1995), however the same accuracy estimates hold.

[1] With intensities of $I(10938)/I(4103) = 9.03/25.95 = 0.348$ and $I(8665)/I(3734) = 0.83/2.41 = 0.344$ for $n_e = 1000\,\mathrm{cm}^{-3}$, T_e = 10 000 K; Hβ = 100 (Storey & Hummer 1995).

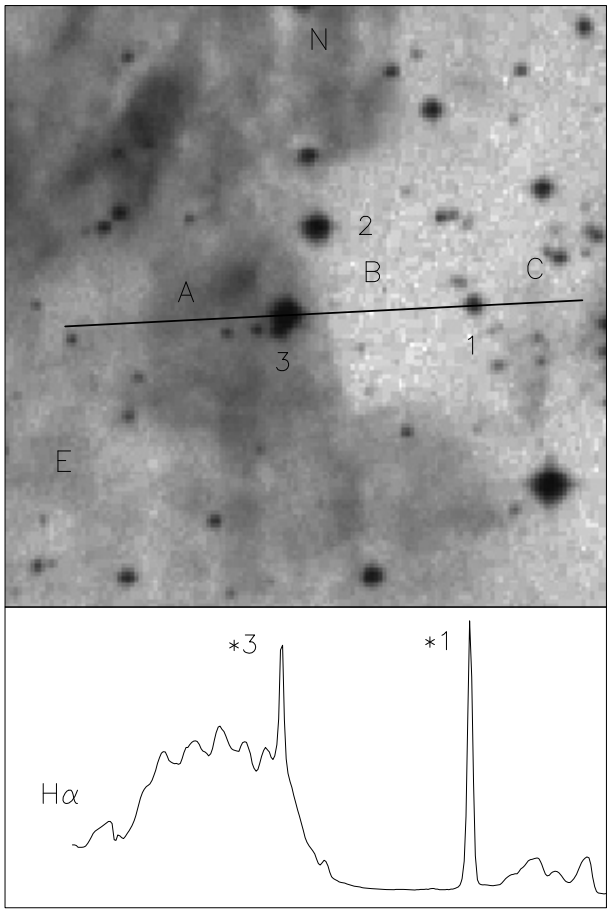

Fig. 1. Part of M 17 and slit sections A, B (3*–1*) and C (Table 2). The stars 1, 2 and 3 observed by Chini et al. (1980) are indicated. The distance between star 1 and 3 is 83″.

4. Observations

4.1. New observations

Our observations of M 8 and M 17 were made with the ESO 1.52-m telescope and the BC-spectrograph in 1st and 2nd order, at a resolution of $\lambda/\Delta\lambda$ = 4500. The spectra were flat-fielded and calibrated against the standard star LTT 7379 (Stone & Baldwin 1983; Baldwin & Stone 1984). The line intensities were extracted from Gaussian profile fits, and the intensities are normalized to $F(\mathrm{H}\beta) = 100$. The accuracy of the observations is ~15%. Our data of M 8 and M 17 are listed in Tables 1 and 2. The M 8 data cover an area of 10″ × 2″ in the Hour-Glass region close to the position HG, where the observations by Sanchez & Peimbert (1991) and Garcia-Rojas et al. (2007) were made. The position of the slit (2″ width) across M 17 is shown in Fig. 1.

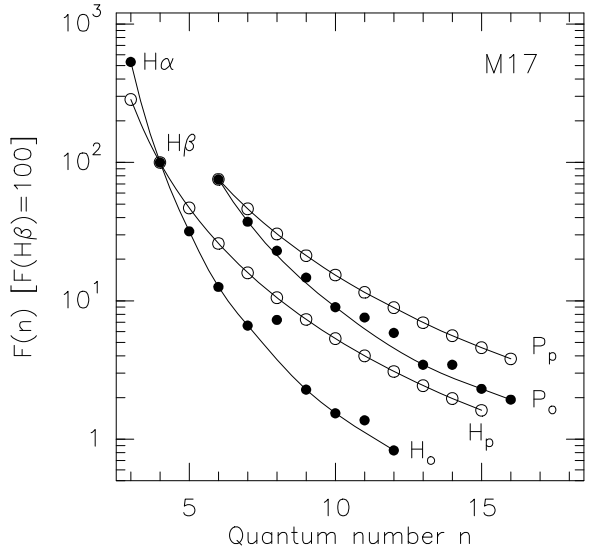

Fig. 2. M 17. Illustration of the smoothness of the Paschen (P) and Balmer (H) decrement. Solid dots: observations (region A, Table 2), open circles: predictions (n_e = 1000 cm^{-3}, T_e = 10 000 K).

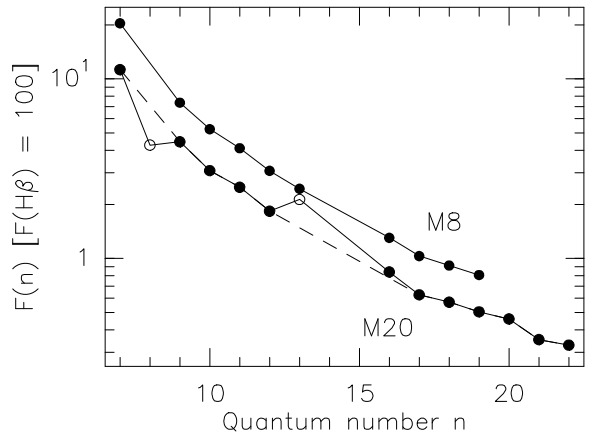

Fig. 3. Observed Paschen decrement of M 8 and M 20 (data from Garcia-Rojas et al. 2006, 2007). Open circles: inconsistent data that were corrected to follow a smooth decrement (dashed line). The lines P8, P13 are not blended by sky emission lines (Table 5).

Figure 2 illustrates the smoothness of the predicted and observed Paschen and Balmer decrement for region A of M 17 (Table 2). The observed Paschen lines P 11, P 12, and P 14 and the observed Balmer lines H 8 and H 11 show some deviation from a smooth decrement, attributed mainly to contamination by sky emission lines in the Paschen line region (for the sky emission lines see Osterbrock & Martel 1992; Hanuschik 2003; Table 5) and to the He I 3889 Å blend of the Balmer H 8 line (Table 5). All observations used in this investigation were checked graphically in this way, and if necessary, corrections were made so that the intensities follow smooth decrements. In Table 2, the data in brackets are corrected in this way, and the corrected values (region A) are used in relation (2).

4.2. Observations by Garcia-Rojas et al. and Esteban et al.

Paschen and Balmer line observations of M 8, M 16, M 17, M 20, NGC 3603, and S 311 are taken from Garcia-Rojas et al. (2005, 2006, 2007). Their observations are based on echelle spectra (3200–10 350 Å), but the lines P 14, P 15, H 8, and H 14 were not observed since they fall in the order separation of the spectra. The accuracy of the observations is 5 to 15%. When applying relation (2) to the observations of M 20, an inconsistent result A_V, R ($100\% < \sigma_A, \sigma_R$) is obtained that can be attributed to some peculiarities of the observed Paschen decrement, as shown in Fig. 3. The inconsistent data were forced to a smooth decrement, and the corrected data are used in relation (2).

The observations of M 42 are taken from Esteban et al. (2004). The 9 line pairs used in the PH-method are between n = 7 and n = 19, while the line pairs n = 8, 10, 14, and 15 were not observed (order separation). Again, the accuracy of the observations is 5 to 15%.

Table 1. Observations of M 8, 10″ × 2″ area of the Hour Glass region HG (see Sanchez & Peimbert 1991).

n	λ	$F(\lambda)/F(\mathrm{H}\beta)$	λ	$F(\lambda)/F(\mathrm{H}\beta)$
	Paschen		Balmer	
4			4861	100
5			4340	36.4
6	10 938	31.4	4103	15.8
7	10 049	18.4	3970	9.66
8	9546	9.35	3889	5.44
9	9229	6.55	3835	3.21
10	9015	4.28	3797	2.18
11	8863	3.27	3770	1.83
12	8750	2.36	3750	1.39

4.3. NGC 7027: observations by Rudy et al. and Zhang et al.

From Rudy et al. (1992) we take the observed emission line ratios P n/P 6 for 6 ≤ n ≤ 14, and from Zhang et al. (2005) we take the observed emission line ratios P n/Hβ for 10 ≤ n ≤ 22 and H n/Hβ for 6 ≤ n ≤ 22. The Paschen line intensities (10 ≤ n ≤ 14) of both observations were compared to arrive at a common intensity scale. The Paschen line P 8 (9545 Å) (Rudy et al. 1992) is not used since it is blended with [SIII] (9532 Å), the corresponding Balmer line H 8 (3889 Å) is blended with He I 3889 Å. The published intensity of H 14 (3721 Å) is blended with [OII] (3727 Å), and the H 16 line may be blended by the line He I 3705 Å. The intensities of H 14 and H 16 were corrected to follow a smooth decrement (correction H 14 from 1.753 to 0.73, H 16 from 0.853 to 0.55). The Paschen and Balmer line intensities obtained in this way are shown in Fig. 4. The accuracy of the combined observations is probably of the order of 25%.

5. Results and notes on individual objects

The values A_V and R derived from the PH-method are compared in Table 3 with determinations from the photometric method (2.1) and (2.2). The uncertainties σ_A, σ_R of the A_V, R determinations are summarized in Table 4. The value R agrees when derived either from the photometric method or the PH-method. Some notes follow on the individual objects.

M 8. For the exciting star Herschel 36 (HD 164740), in the Hour-Glass region of M 8, the value R = 4.6–5.6 was derived by Hecht et al. (1982) and R = 5.3 by Cardelli et al. (1989), while Sanchez & Peimbert (1991) use R = 5.0. The PH-method applied to our observation (Table 1, 7 line pairs) of the emission region close to Her 36 gives A_V = 2.3 mag and R = 4.35. The PH-method applied to the observation of Garcia-Rojas et al. (2007) of the same region gives the values A_V = 2.2 mag and R = 6.1 for the 11 line pairs between 7 ≤ n ≤ 20. It is necessary

Table 2. Observation of M17 (Fig. 1).

n	Wavelength		$F(\lambda)/F(\mathrm{H}\beta)$ region A		$F(\lambda)/F(\mathrm{H}\beta)$ region B		$F(\lambda)/F(\mathrm{H}\beta)$ region C		$F(\lambda)/F(\mathrm{H}\beta)$ region N 3	
	P	H	P	H	P	H	P	H	P	H
3	–	6563	–	532	–	1102	–	667	–	510
4	–	4861	–	100	–	100	–	100	–	100
5	–	4340	–	31.8	–	22.3	–	32.0	–	29.78
6	10 938	4103	75.4	12.6	–	11.4	–	11.6	–	11.27
7	10 049	3970	37.3	6.62	250	6.7	141	(6.5)	–	–
8	9546	*3889	23.0	7.28 (3.86)	256	–	79.9	–	–	–
9	9229	3835	14.7	2.28	82.7	–	51.79	–	12.6	1.51
10	9015	3797	9.00	1.54	43.5	–	16.22	–	7.71	0.98
11	8863	3770	7.57 (6.29)	1.37 (1.12)	33.3	–	–	–	–	–
12	8750	3750	5.86 (4.47)	0.94	29.6	–	–	–	–	–

Notes. * Blend with HeI 3889 Å. Values in bracket: corrected to obtain a smooth decrement (Fig. 2).

Table 3. Determination of A_V, R from common upper level PH lines, and R derived from stellar photometry.

	PH Emission Lines					Stellar Photometry		
Object	Obs.[a]	PH Pairs[b]	A_V(mag)	R[c]	A_V(Hα–Hβ)[d]	Star/Cluster	R	Ref.
M 8	TP	7 [6–12]	2.10	4.35		Herschel 36	4.6–5.6, 5.3	2, 3
	G-R	11 [7–20]	2.20	6.1 (5.0)[e]	2.1(1.4)	NGC 6523	4.6	4
M 16	G-R	9 [7–18]	2.80	5.2 (3.1,4.8)[f]	3.2(2.3)	NGC 6611	4.8	5
M 17	TP	7 [6–12]	3.50	4.1	2.35(2.0)	NGC 6618	4.2	1
	G-R	9 [7–18]	3.05	4.3 (3.1)	3.4(2.7)	Star 1 (Fig. 1, 5)	4.5 ± 0.25	TP
M 20	G-R	14 [7–22]	1.05	5.5 (3.1)	0.8(0.8)	HD 164492	5.1	6, 7
						HD 164492	3.1	8
M 42	E	9 [7–19]	2.15	5.8	2.2(1.5)	θ^1 Ori C	5.5	9
NGC 3603	G-R	8 [9–18]	6.9	5.4 (3.1)	7.4(5.5)	NGC 3603	4.3	10
S 311	G-R	10 [7–18]	1.90	5.5 (3.1)	2.1(1.5)	[NGC 2467	1.8–3.9]	11
NGC 7027	Z-R	16 [6–22]	3.9	4.4 (3.1)[g]	4.0 (3.1)			

Notes. [a] Observer, TP: this paper, G-R: Garcia-Rojas et al. (2005, 2006), E: Esteban et al. (2004), Z-R: Zhang et al. (2005) and Rudy et al. (1992). [b] Number of line pairs, in brackets the range of quantum numbers considered. [c] Determined from relation (2); values in brackets used by G-R. [d] From Hα–Hβ ratio and R of Col. 5; in brackets for $R = 3.1$. [e] For 4100 Å $< \lambda$, for shorter λ see Garcia-Rojas et al. (2007). [f] $R = 3.1$ for 5500 Å $< \lambda$, $R = 4.8$ for $\lambda < 5500$ Å. [g] Value usually taken.
References. 1: Chini et al. (1980), Chini & Krügel (1983), Hoffmeister et al. (2008); 2: Hecht et al. (1982): 4.6–5.6; 3: Cardelli et al. (1989): 5.0; 4: McCall et al. (1990); 5: Chini et al. (1980), Chini & Wargau (1990), Chini et al. (1992); 6: Anderson (1970); 7: Lynds et al. (1985); 8: Kohoutek et al. (1999); 9: Cardelli & Clayton (1988); 10: Pandey et al. (2000); 11: Grubissich (1969), NGC 2467 may not be a physical cluster.

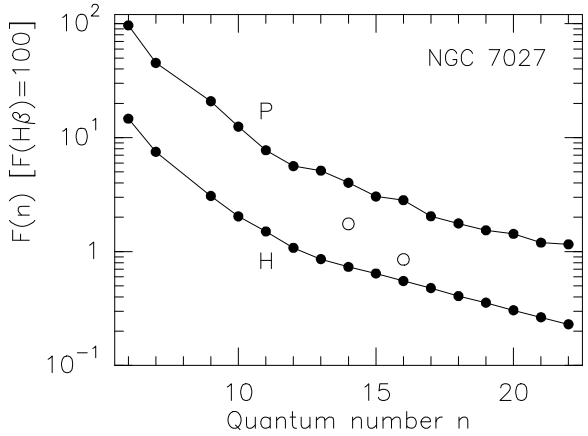

Fig. 4. Paschen (P) and Balmer (H) decrement of NGC 7027, based on observations of Rudy et al. (1992) and Zhang et al. (2005). The published intensities of the Balmer lines $n = 14$ and $n = 16$ (open circles) are corrected to follow a smooth decrement.

to consider the value $R = 6.1$ with some caution because of inconsistencies between the Garcia-Rojas et al. (2007) Balmer line measurements (for $\lambda < 4100$ Å) compared to those of Esteban et al. (1999), while the observation by Esteban et al. does not provide a solution A_V, R, probably because of the stated difficulties of the P8 to P11 line calibration as explained in both publications. Finally, the measurements by McCall et al. (1990) cover stars in an area of several 10′, so that their value $R = 4.6$ is the average over a large area (method 2.1).

M 17 . The values A_V, R do not change when leaving out in the least-square fit the line pair P8/H8, instead of using the corrected ratio from a smooth decrement (Fig. 2).

Figure 1 shows that Star 1 observed by Chini et al. (1980) is covered by the slit. Figure 5 is the spectral distribution of Star 1 measured by us at the wavelengths listed for the standard star LTT 7379 (Stone & Baldwin 1983; Baldwin & Stone 1984). Star 1 is assumed to have the spectral type O 4 V (Chini et al. 1980), and the catalogued spectral distribution (Pickles 1998) of a very similar O 5 V star is inserted in Fig. 5. The O 5 V star was taken since the catalogued spectral distribution extends to 10 400 Å. Using the value $R = 4.2$, obtained from the two-colour diagram of the cluster NGC 6618, for Star 1, Chini et al. (1980) derived the extinction $A_V = 9.2$ mag towards this star. Applying method (2.2) to all data points of the observation shown in Fig. 5 a, we obtain the values $A_V = 10.4$ mag ($\sigma_A = 3\,\%$) and $R = 4.5$ ($\sigma_R = 5\,\%$) for Star 1. The value $R = 4.5$ agrees well with the value $R = 4.1$ derived from the PH-method applied to the lines of the nearby emission region (Fig. 1). Figure 5 b

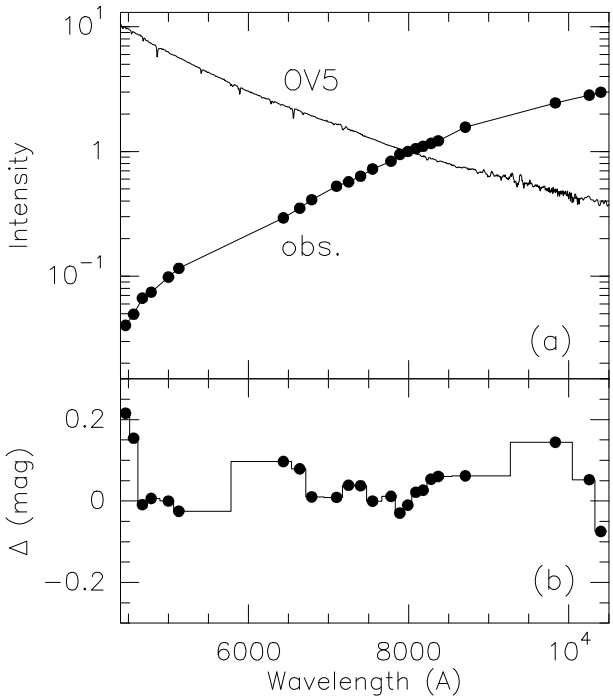

Fig. 5. a) Observation (dots) of Star 1 in M 17 (Fig. 1), classified by Chini et al. (1980) to be of spectral type O4 V. Continuous line: spectral distribution of a non-reddened O5 V star, taken from Pickles (1998). The data are normalized at 8000 Å. **b)** Magnitude difference between the O5 V star, reddened by $A_V = 10.4$ mag, $R = 4.5$, and the observation of Star 1.

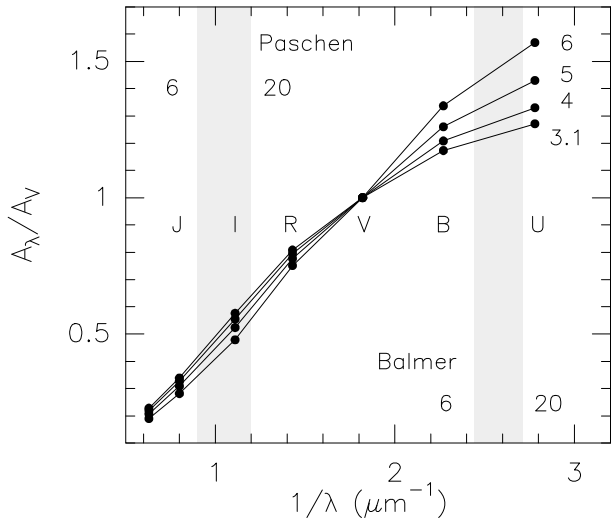

Fig. 6. Position of the Paschen and Balmer lines ($6 \le n \le 20$) with respect to the linear near-IR part of the reddening curve and the blue part that is sensitive to R (values $R = 3.1, 4, 5, 6$). The reddening curve is the parametrized form of relation (1) (Cardelli et al. 1989).

shows that the CCM reddening curve can be applied in this region of M 17.

Star 3 is located at the edge of region A of strong emission (Fig. 1), which did not allow the derivation of a clean spectral distibution of the reddened star. From the ratios P 9/H 9 and P 10/H 10 measured in the nebular region N 3 near Star 3 (Table 2), together with the value $R = 4.2$, we obtain $A_V = 4.0$ mag, which compares well with the value $A_V = 3.7$ mag derived by Chini et al. (1980) for this star.

The emission line intensities of M 17 (position 14) published by Garcia-Rojas et al. (2006), and used here, are for a region ∼4′ to the east of the cluster NGC 6618 and ∼2′ to the east of Star 3 in Fig. 1. The value R seems to be constant over a large area of the nebula.

M 20 . There is contradictory information for the value R in the direction of the central star HD 164492 in M 20. Anderson (1970) and Lynds et al. (1985) use $R = 5$, while Kohoutek et al. (1999) use $R = 3.1$, although they did not make a new determination of R. Garcia-Rojas et al. (2007) use $R = 3.1$. The data of Fig. 3 show deviations of the P 8, P 13, and P 16 intensities from a smooth Paschen decrement, while the observations of the Balmer lines (not shown) follow a smooth decrement. When correcting the observation of Garcia-Rojas et al. (2007), i.e. P 8 from 4.274 to 6.73, P 13 from 2.131 to 1.41 and P 16 from 0.84 to 0.77, and using in relation (2) the 14 line pairs between $7 \le n \le 22$, the result is $A_V = 1.0$ mag and $R = 5.5$.

Again, when leaving out in the least-square fit the line pairs P8/H8 and P13/H13 instead of using the corrected values (Fig. 3), the solution is $A_V = 1.2$ mag ($\sigma_A = 19\,\%$), $R = 6.7$ ($\sigma_R = 33\%$, Table 4). However, the range $R \pm \sigma_R$ is wide for both cases, and contains both values R.

M 42. The emission line spectrum published by Esteban et al. (2004) is taken at 27″ from the Trapezium star θ^1 Ori C. Cardelli & Clayton (1988) derived $R = 5.50$ and $E(B-V) = 0.34$ in the direction of this star. This gives $A_V = 0.34 \times 5.50 = 1.9$ mag. For an earlier determination of R between 4.4 and 7.7 for the Orion nebula region see Costero & Peimbert (1970).

NGC 3603. Pandey et al. (2000) published $R = 4.3 \pm 0.2$ as best value, mainly based on UBV photometry of cluster stars. Their paper illustrates the sensitivity of the value R on the photometric data set and the method of analysis.

S 311. The H II region S 311 is excited by the star HD 64315 of type O 6 Vnne (Gamen et al. 2006). HD 64315 belongs to the cluster NGC 2467, which, however, seems to be a superposition of early-type stars rather than a true physical cluster (Feinstein & Vazquez 1989). Grubissich (1969) suggests that the value of R lies between 1.8 and 3.9 for NGC 2467. The colour excess of HD 64315 is $E(V-B) = 0.54$, which gives the extinction $A_V = 1.7$ mag for $R = 3.1$, and the value $A_V = 3.0$ mag for $R = 5.5$ derived from the PH-method (Table 3).

NGC 7027. The planetary nebula NGC 7027 is associated with dust (see for instance Seaton 1979; Middlemass 1990; Sanchez Contreras et al. 1998); however, to derive the extinction A_V, the standard value $R = 3.1$ is generally used. Application of the PH-method with the predicted ratio $R_p = 0.31$ (Sect. 3) to the data shown in Fig. 4 gives $A_V = 3.9$ mag and $R = 4.4$ if using the 16 line pairs between $6 \le n \le 22$. The same values A_V, R are obtained when leaving out the inconsistent line pairs P14/H14 and P16/H16 instead of using the corrected measurements (Fig. 4). If the low-density/low-temperature ratio $R_p = 0.345$ (Sect. 3) were used, the values would be $A_V = 3.7$, $R = 4.5$, illustrating the small dependence of the PH-method on n_e, T_e, i.e. R_p, of the nebula.

6. Observational and astrophysical aspects of the PH-method

6.1. Sky lines, line blends, instrumental sensitivity

The common upper level PH lines are weak so that elimination of sky lines and nebular line blends is important. Table 5

Table 4. Accuracy of A_V, R determination.

Object	PH-method N^a	A_V (mag)	σ_A (%)	R	σ_R (%)	Photometry[b] R	quoted error (%)	Method (Sect. 2)
M 8	7	2.1	11	4.35	21	4.6	±6	2.1
	11	2.2	7	6.1	11	4.6–5.6, 5.3		2.2
M 16	9	2.8	6	5.2	10	4.8	±4	2.1
M 17	7	3.5	4	4.1	7	4.2–4.9	±6–9	2.1
	9	3.05	11	4.3	17	4.5	5	2.2, Fig. 5
M 20	14	1.05	20	5.5	33	5.1		2.2
M 42	9	2.15	9	5.8	15	5.5		2.2
NGC 3603	8	6.9	6	5.4	10	4.3	±5	2.1
S 311	10	1.9	19	5.5	33			
NGC 7027	7	3.9	6	4.4	8			

Notes. [(a)] Number of lines used in PH-method. [(b)] See Table 3 for references.

Table 5. Line strengths, sky line blends, emission line blends (Hβ = 100).

n	Pn	I(Pn)/Hβ	Blend (sky)[a] OH (v'–v'')	Hn	I(Hn)/Hβ	Blend[b]
6	10 938	9		4101	26	
7	10 049	5.5		3970	16	
8	9545	3.5		3889	10	He I 3889 (15.0)*
9	9229	2.5		3835	7	He I 3834 (0.06)
10	9015	1.8		3798	5	[SIII] 3799 (5.4)*
11	8863	1.4	8867(7–3)	3770	4	He I 3769 (0.02)
12	8750	1.1		3750	3	O II 3749 (0.12)
13	8665	0.8		3734	2.5	He I 3733 (0.05)
14	8598	0.7	8597(6–2)	3721	2	[OII] 3726,3729 (56)* [SIII] 3721
15	8545	0.5	8549(6–2)	3712	1.5	O II 3713 (0.03), Ne II 3713 (0.05)
16	8502	0.45	8505(6–2)	3703	1.3	He I 3705 (0.7)*
17	8467	0.4	8465(6–2)	3697	1.1	
18	8438	0.3		3691	1.0	
19	8413	0.3	8415(6–2)	3686	0.8	
20	8392	0.25		3683	0.7	

Notes. [(a)] From Osterbrock & Martel (1992). [(b)] Nebular emission line, strong line: *; in brackets: line strength in the Orion nebula (Esteban et al. 2004).

indicates that the intensity of the Pn and Hn lines (for $6 \lesssim n \lesssim 20$) are between ~30% and 1% of Hβ (=100). The table also indicates that the weaker Pn lines are located in the region of many OH sky emission lines (Osterbrock & Martel 1992; Hanuschik 2003), often of equal strength as the nebular emission lines, while there are hardly any nebular emission line blends in the red wavelength region. The Hn lines of the blue wavelength region are relatively strong, while the sky lines in this wavelength region are very weak (Osterbrock et al. 1996; Hanuschik 2003, his Fig. 5). The lines H8, H10, H14, and H16 (see Table 5) coincide with strong nebular emission lines. A high spectral resolution and off-source sky background exposures are required. The atmospheric extinction is measured on a nearby standard star.

The common upper level Pn–Hn lines are outside the maximum response of commonly used CCD detectors; however, the sensitivity of any observation of the Pn-Hn lines also depends on the aperture of the telescope and the resolution of the spectrograph. Typical values of CCD efficiencies are ~80–90% for the Hα–Hβ region, ~35–60% for the 3500–4000 Å region and ~60–10% for the 8500–11 000 Å region. It is difficult to obtain good measurements of the P6 10 938 Å line, though the data of Tables 1 and 2 contain reliable values (accuracy <25 %).

6.2. Photometric method versus PH-method

There are two differences between any line ratio method (for instance Hα/Hβ ratio or PH-method (2.3)) and the photometric methods ((2.2), (2.2)):

(a) the photometric methods are not affected by light scattered in the nebula (see Osterbrock 1989; Krügel 2009), so that the photometric methods can be summarized as the slab-screen extinction method;
(b) the line ratio method uses observed emission line intensities (or fluxes) that are affected by (1) internal extinction and scattering in the emission nebula itself, (2) possible back scattering on the rear surface of the emission nebula, and (3) external extinction and scattering in a slab-screen in front of the nebula. These effects apply to all line ratio methods, and are not a particularity of the PH-method. There are many studies that calculate (estimate) these effects; for instance, for (1) see Mathis (1970, 1972, 1983), for (2) see O'Dell et al. (1992), for (3) see Natta & Panagia (1984), Osterbrock (1989), and others. A general conclusion of these studies is, that from measured line ratios and their spatial variation, it is difficult to decide in which proportion the effects (1)−(3) do occur, unless one has recourse to radio and emission line flux meaurements (see for instance

Mathis 1983; Caplan & Deharveng 1986). From radiative transfer calculations of several models of emission nebulae, scattering functions and albedos of the dust grains, and especially applied to the common upper level line ratio P6/H6, Mathis (1970) concludes that "the assumption that all dust is external to a nebula is very good for determining relative line strengths for wavelengths between those for which the extinction correction was determined. As [his] Table 3 shows, the errors are not worse if the [extinction] correction is determined from Hα/Hβ instead of P6/H6".

Throughout this paper we have used the CCM parameterized extinction law. This may not necessarily be the most appropriate extinction law for a particular emission nebula, as suggested for the Orion nebula (M 42) by Bautista et al. (1995), although their conclusion needs to be confirmed. We have also assumed, as is usually done, that Case B applies to the emission nebulae discussed here.

7. Summary

The position of the Paschen lines Pn and Balmer lines Hn, for $6 \leq n \leq 20$, with respect to the reddening curve is illustrated in Fig. 6. The Paschen lines cover the linear part of the reddening curve, and the Balmer lines cover the blue section that is sensitive to the actual value R.

The PH-method of extinction determination A_V, R exploits the favourable fact that the predicted intensity ratios $R_p(n)$ of common Paschen-Balmer lines are nearly insensitive to the excitation condition n_e, T_e of the emission nebula. The ratios $R_p(n)$ are constant within ~5% for different levels n at given n_e, T_e, and constant within ~10% for the range from low-density/low-temperature emission nebulae ($R_p(n) = 0.34$) to high-density/high-temperature planetary nebulae ($R_p(n) = 0.31$). The accuracy of the PH-method depends therefore primarily on the accuracy of the observations. The consistency of the observation/data reduction can be checked because the observed lines must show a smooth Paschen and Balmer decrement.

We have shown for 6 emission nebulae (Table 3) that the extinction A_V and the total-to-selective absorption R are easily derived from the common Paschen-Balmer line method (2.3), and that the values agree with those derived from the photometric methods (2.1) and (2.2) of associated stars and/or stellar clusters, keeping in mind that the value R derived from the photometric method (2.1) is the average over the extended star cluster region.

The PH-method can be used for emission nebulae and planetary nebulae where no stars are available for photometry. It is worth noting that for the emission nebulae and the planetary nebula of Table 3 the values R are higher than ~4, thus higher than the value $R = 3.1$ of the diffuse interstellar medium that is often used because of lack of exact knowledge. The PH-method opens the possibility of investigating emission nebulae in a more systematic and extended way for their actual values R. The PH-method can be used for mapping of the value R across nebulae and – when using large telescopes – investigation of extra-galactic emission nebulae in near-by galaxies, such as the LMC, SMC, M 31, and M 51.

The PH-method gives the value R for the entire wavelength region between ~3700 Å and 10 400 Å. The PH-method does not allow any investigation of a different value R of, for instance, the blue wavelength region and the red wavelength region as applied by Garcia-Rojas et al. (2006, 2007) to M 8 and M 16. The PH-method relies on precise measurements of the Balmer lines (5 to 10% accuracy) since the lines of the blue wavelength region are sensitive to the actual value of R (see Fig. 6).

Acknowledgements. For the line ratios we used Storey & Hummer's programme inrat.f, retrieved from the CDS. We thank the referee (G. C. Clayton) for his comments, and in particular for the remarks that resulted in adding Sect. 6 summarizing the observational and astrophysical aspects of the PH-method.

References

Anderson, C. M. 1970, ApJ, 160, 507
Baldwin, J. A., & Stone, R. P. S. 1984, MNRAS, 206, 241
Bautista, M. A., Pogge, R. W., & DePoy, D. L. 1995, ApJ, 452, 685
Bevington, P. R., & Robinson D. K. 2003, Data Reduction and Error Analysis (Boston, New York, San Francisco: McGraw Hill)
Brocklehurst, M. 1971, MNRAS, 153, 471
Caplan, J., & Deharveng, L. 1986, A&A, 155, 297
Cardelli, J. A., & Clayton, G. C. 1988, AJ, 95, 516
Cardelli, J. A., Clayton, G. C., & Mathis, J. S. 1989, ApJ, 345, 245 (CCM)
Chini, R., & Krügel, E. 1983, A&A, 117, 289
Chini, R., & Wargau, W.F. 1990, A&A, 227, 213
Chini, R., Elsässer, H., & Neckel Th. 1980, A&A, 91, 186
Chini, R., Krügel, E., & Wargau, W.F. 1992, A&A, 265, 45
Costero, R., & Peimbert, M. 1970, Bol. Obs. Tonantzintla y Tacubaya, 5, 229
Esteban, C., Peimbert, M., Torres-Peimbert, S., Garcia-Rojas, J., & Rodriguez, M. 1999, ApJS, 120, 113
Esteban, C., Peimbert, M., Garcia-Rojas, J., et al. 2004, MNRAS, 355, 229
Feinstein, A., & Vazquez, R.A. 1989, A&AS, 77, 321
Gamen, R. C., Barba, R., Rubio, M., Mendez, R. A., & Minniti, D. 2006, Rev. Mex. Astron. Astrofis. Conf. Ser., 26, 72
Garcia-Rojas, J., Esteban, C., Peimbert, A., et al. 2005, MNRAS, 362, 301
Garcia-Rojas, J., Esteban, C., Peimbert, M., et al. 2006, MNRAS, 368, 253
Garcia-Rojas J., Esteban C., Peimbert A., et al. 2007, Rev. Mex. Astron. Astrofis., 43, 3
Goudis, C. 1982, The Orion Complex: A case study of interstellar matter, (Dordrecht: Reidel)
Greve, A., Castles, J., & McKeith, C. D. 1994, A&A, 284, 919
Grubissich, C. 1969, A&A, 2, 245
Hanuschik, R. W. 2003, A&A, 407, 1157
Hecht, J., Helfer, H. L., Wolf, J., Donn, B., & Pipher, J. L. 1982, ApJ, 263, L39
Hoffmeister, V. H., Chini, R., Scheyda, C. M., et al. 2008, ApJ, 686, 310
Kohoutek, L., Mayer, P., & Lorenz, R. 1999, A&S, 134, 129
Krügel, E. 2009, A&A 493, 385
Lynds, B. T., Canzian, B. J., & O'Neil, E. J. 1985, ApJ, 288, 164
Mathis, J. S. 1970, ApJ, 159, 263
Mathis, J. S. 1972, ApJ, 176, 651
Mathis, J. S. 1983, ApJ, 267, 119
Mathis, J. S. 1990, ARA&A, 28, 37
McCall, M. L., Richer, M. G., & Visvanathan, N. 1990, ApJ, 357, 502
Middlemass, D. 1990, MNRAS, 244, 294
Natta, A., & Panagia, N. 1984, ApJ, 287, 228
O'Dell, C. R., & Wen, Z. 1992, ApJ, 387, 229
O'Dell, C. R., Walter, D. K., & Dufour, R. 1992, ApJ, 299, L 67
Osterbrock, D. E. 1989, Astrophysics of Gaseous Nebulae and Active Galactic Nuclei (Mill Valley, CA, USA: University Science Books)
Osterbrock, D. E., & Martel, A. R. 1992, PASP, 104, 76
Osterbrock, D. E., Fulbright, J. P., Martel, A. R., et al. 1996, PASP, 108, 277
Pandey, A. K., Ogura, K., & Sekiguchi, K. 2000, PASJ, 52, 847
Pickles, A. J. 1998, PASP, 110, 863
Rudy, R. J., Erwin, P., Rossano, G. S., & Puetter, R. C. 1992, ApJ, 384, 536
Sanchez, L. J., & Peimbert, M. 1991, Rev. Mex. Astron. Astrofis., 22, 285
Sanchez Contreras, C., Alcolea, J., Bujarrabal, V., & Neri, R. 1998, A&A, 337, 233
Seaton, M. J. 1979, MNRAS, 187, 785
Stone, R. P. S., & Baldwin, J. A. 1983, MNRAS, 204, 347
Storey, P. J., & Hummer, D. G. 1995, MNRAS, 272, 41
Whittet, D. C. B. 2003, Dust in the Galactic Environment, Series in Astronomy and Astrophysics
Zhang, Y., Liu, X.-W., Luo, S.-G., Pequignot, D., & Barlow, M. J. 2005, A&A 442, 249